

Numerical simulation of rotational flow in hydrocephalic hydro-elastic models

¹Hemalatha Balasundaram, ²Senthamilselvi Sathyamoorthi, ³Ambrose Prabhu R, ⁴Shyam Sundar Santra

^{1,3}Rajalakshmi Institute of Technology, Chennai, Tamilnadu, India.

²Vels University, Pallavaram, Chennai, Tamilnadu, India.

⁴Department of Mathematics, JIS College of Engineering, Kalyani, West Bengal 741235, India

Abstract

Three-dimensional computational models of the cerebrospinal fluid (CSF) flow and brain tissue are presented for evaluation of their hydrodynamic conditions before and after shunting for seven patients with non-communicating hydrocephalus. We have developed a mathematical model of the fluid flow in cerebral ventricles during hydrocephalus is presented. The fluid-solid interaction simulation shows the CSF mean pressure is five times greater than normal subject. We present a brief overview of the clinical problems that are being addressed. This suggests that functional deficits observed in hydrocephalic patients could therefore be more related to the damage to periventricular white matter.

Introduction

Many researchers have constructed the computational theory of hydrocephalus based on poro-elasticity. Such models would provide greater comprehension of the problem and, as a result, better therapy. Such models have also neglected to account for the intermittent effects of shunting, the most often utilized treatment for hydrocephalus. We use elasticity and fluid mechanics to create a mathematical model of the human brain and ventricular system. Our model expands previous work by considering flow across the aqueduct and including boundary constraints. This would create a quantitative model for the disorder's boundary and improvement. We develop and solve the governing equations and boundary conditions for this model along with meaningful clinical findings.

Our model expands earlier research on hydrocephalus by incorporating aqueduct flow with boundary constraints. A Cerebrospinal fluid travels down the subarachnoid space around the spinal cord and then into the cranial subarachnoid space, however, the laws of physics make it difficult to explain how this flow could be endured.

A mathematical methodology that utilized in vivo stimuli was used to study the dynamic interplay of pulsatile blood, brain, and CSF¹. The simulation presented in this article was generated for individuals with CSF physio pathological illness hydrocephalus². An investigation of the posterior ventricular permeability for an asymmetrical circulation with chemical concentration for idiopathic hydrocephalus³. Using a basic geometric model, the current work presents an entirely novel approach to multi-physical diffusion processes in hydrocephalus and serves as a standard for more geometrically sophisticated simulations⁴. The circulation of CSF in the cardiovascular and sub-arachnoidal routes and CSF seepage into the

porous brain parenchyma were addressed. The complicated brain geometry's boundary conditions were developed⁵.

A standard subject's study information has been compared to an actual computational model that represented intracranial dynamics. The model, which was created utilizing subject-specific magnetic resonance (MR) images and physical boundary conditions as input, reproduces pulsating CSF circulation and simulates intracranial pressures and flow rates⁶. The numerical model was used to explore how cross-sectional geometry and spinal cord motion affect unsteady velocity, shear stress, and pressure gradient fields⁷. The system was broken down into five submodels: blood from the arterial system, blood from the venous system, ventricular CSF, cranial subarachnoid space, and spinal hemorrhagic space. Resistance and compliance connect these submodels. The constructed model was utilized to mimic key functional features found in seven healthy individuals, such as arterial, venous, and CSF flow distribution (amplitude and phase shift)⁸.

Previously, time-resolved three-dimensional magnetic resonance velocity mapping was utilized to study healthy and abnormal blood flow patterns in the human vascular system. This approach was utilized to investigate the temporal and spatial variations of CSF flow in the ventricular system of 40 healthy volunteers⁹.

The barrier between CSF and blood in these granulations is minimal, allowing CSF to flow into the circulation and be absorbed. In contrast to CSF production, consumption is pressure-dependent, with the rate influenced by the differential between intraventricular and superior sagittal venous pressure. In the present study, these effects and ICC diagrams have been investigated using 3D FSI simulation up to 2.5 years after shunt surgery in a large number of NCH patients through a non-invasive method¹⁰.

A finite element parametric investigation on a head model under different scenarios of impact is conducted. In the study, the CSF material parameters are varied within the expected range of change, while other components of the head model are kept constant¹¹.

In this chapter, we construct a model of the cerebral cortex and circulatory system that is complex enough to imitate the behavior of a hydrocephalic brain while being simple enough to be computationally accessible, and then we employ it to analyze the disorder's genesis and therapy. CSF perfusion throughout the human brain system has oscillatory fluid dynamics. The cardiac area has been demonstrated within a porous material with suitable pulsatile boundary conditions. This simulation was developed for people with CSF physiopathological disease hydrocephalus. We computed the cerebral bloodstream circulation rate of patients using acceptable validity.

Mathematical Formulation

In this study, the CSF is treated as a Newtonian fluid, with dynamic viscosity and density of 1.003×10^{-3} kg/ms and 998.2 kg/m³, respectively [1]. The brain tissue is a linearly viscoelastic substance, with storage and dissipation parameters of 2038 and 1356 Pa for individuals in good health, 1594 and 1015 Pa for patients, respectively, and a density of 1040 kg/m³ [8, 9]. CSF flow rate in the lateral ventricles is 0.35 cm³/min [1]. For numerical models, this number is employed as the value of the amplitude in the input fluids pulsatile flow rate function—the final segment of the ventricular system following the fourth ventricle is chosen as the flow

output site. The usual baseline CSF pressure was established at 500 Pa, whereas the pathological baseline was set at 2700 Pa [6].

$$\frac{\partial u_c}{\partial x} + \frac{\partial w_c}{\partial y} = 0$$

$$\frac{\partial u_c}{\partial t} + Gw_0 \frac{\partial u_c}{\partial y} + 2\Omega'w_c = -\frac{1}{\rho} \frac{\partial p}{\partial x} + \nu \left(\frac{\partial^2 u_c}{\partial y^2} \right) - \frac{RN}{\rho} u_c$$

$$\frac{\partial u_c}{\partial t} + Gw_0 \frac{\partial w_c}{\partial y} - 2\Omega'u_c = -\frac{1}{\rho} \frac{\partial p}{\partial x} + \nu \left(\frac{\partial^2 w_c}{\partial y^2} \right) - \frac{RN}{\rho} w_c$$

$$u_c = \omega \left(\cos \omega t + \frac{1}{2} \sin \omega t \right), w = 0, \text{ at } y = 0 \text{ and } t \leq 0$$

$$u = u_0 \omega, w = 0 \text{ at } y = 1, t > 0$$

Let's consider the pressure difference exponentially transverse concerning angular velocity $\frac{\partial p}{\partial x} = \omega e^{-\omega t}$. We used pulsatile inlet boundary condition [14] to approach the CSF flow in the parenchymal layer. The dimensionless quantities for the above equations by neglecting the dash for our convenience

$$y' = \frac{y}{l}, t' = \frac{tw_0}{l}, w' = \frac{wl}{w_0}, u_c' = \frac{u_c}{u_0}, \omega' = \frac{\omega l^2}{\nu}$$

$$\theta' = \frac{T - T_c}{T_0 - T_c}, Re = \frac{w_0 l}{\nu}, G_{pm} = \frac{RNl^2}{\mu}, \Omega' = \frac{\Omega l^2}{\nu}$$

u and w represent the CSF velocity of the fluid in x & y direction respectively. w_0 represents velocity. Density of CSF is denoted as ρ . Da and Ω are represented as darcy number and angular velocity, G_{pm} referred as particle mass parameter. ω denotes CSF Womersley number.

The above governing equations dimensionalised and hence the dimensionless form of the same with suitable boundary conditions is represented as follows

$$Re \left(\frac{\partial u_c}{\partial t} + G \frac{\partial u_c}{\partial y} \right) + 2\Omega w_c = -\alpha^2 e^{\varphi t} + \frac{\partial^2 u_c}{\partial y^2} - G_{pm} u_c \quad (1)$$

$$Re \left(\frac{\partial w_c}{\partial t} + G \frac{\partial w_c}{\partial y} \right) - 2\Omega w_c = -\alpha^2 e^{\varphi t} + \frac{\partial^2 w_c}{\partial y^2} - G_{pm} w_c \quad (2)$$

$$u_c = \alpha^2 \left(\cos \varphi t + \frac{1}{2} \sin \varphi t \right), w_c = 0 \text{ at } y = 0$$

$u_c = \alpha^2 \cos n\varphi t, w = 0 \text{ at } y = 1$. Where n being an integer.

To solve the above momentum equation the complex function $F_c = u + iw$ where u and w are functions of x and y , Navier Stoke's equation in an explicit form of complex function with boundary conditions is followed as

$$Re \left(\frac{\partial F_c}{\partial t} + G \frac{\partial F_c}{\partial y} \right) + 2\Omega I F_c = -2I\alpha^2 e^{\varphi t} + \frac{\partial^2 F_c}{\partial y^2} - G_{pm} F_c \quad (3)$$

$$F_c = \alpha^2 \left(\cos \varphi t + \frac{1}{2} \sin \varphi t \right), y = 0, t \leq 0$$

$$F_c = \alpha^2 \cos n\varphi t, y = 1, t > 1$$

METHOD OF SOLUTION

We use analytical tools and a model issue to understand the biologically beneficial nature of the cranial systems and their physical consequences. The statistical approach may improve the efficacy of the numerical method. Consequently, we simplify those equations into ordinary differential equations and solve them using perturbation methods. We solve the governing equation utilizing the perturbation approach as it is error-free, adopting the trial solution for velocity.

$$F_c(y, t) = F_0(y) + \frac{\epsilon}{2} e^{i\lambda t} F_1(y) + \frac{\epsilon}{2} e^{-i\lambda t} F_2(y) \quad (4)$$

λ denotes oscillation frequency and ϵ an arbitrary constant with $\epsilon \ll 1$. Consider u_0, u_1, u_2 refers base part, perturbed part of first order and perturbed part second orders of conservation of momentum respectively. F and u 's complex parameters are encoded by I, i .

The analytical perturbation strategy is used to solve the given problem, yielding

$$F_0 = \alpha^2 e^{m_1 y} - A_2 (e^{m_1 y} - e^{m_2 y}) + \frac{2\alpha^2}{a} (e^{m_1 y} - 1) \quad (5)$$

$$F_1 = \alpha^2 \left(\cos \varphi t + \frac{1}{2} \sin \varphi t \right) e^{m_3 y} - \frac{(e^{m_3 y} - e^{m_4 y})}{(e^{m_3} - e^{m_4})} \left[\alpha^2 \left(\cos \varphi t + \frac{1}{2} \sin \varphi t \right) e^{m_3} - \alpha^2 \cos \varphi t + \frac{2\alpha^2 e^{\varphi t}}{b} (e^{m_3} - 1) \right] + \frac{2\alpha^2}{a} (e^{m_1 y} - 1) \quad (6)$$

$$F_2 = \alpha^2 \left(\cos \varphi t + \frac{1}{2} \sin \varphi t \right) e^{m_5 y} - \frac{(e^{m_5 y} - e^{m_6 y})}{(e^{m_5} - e^{m_6})} \left[\alpha^2 \left(\cos \varphi t + \frac{1}{2} \sin \varphi t \right) e^{m_5} - \alpha^2 \cos \varphi t + \frac{2\alpha^2 e^{\varphi t}}{b} (e^{m_5} - 1) \right] + \frac{2\alpha^2}{a} (e^{m_1 y} - 1) \quad (7)$$

RESULT AND DISCUSSION

To investigate the different physical characteristics such as dynamic viscosity, density, kinematic viscosity, resistance parameter, Elastic parameter, Reynolds number, and Womersley number were calculated analytically and the results are shown below. The intracranial pressure of normal subject human beings was found to be 500Pa and 3000Pa for hydrocephalus patients [14]. The size of the lateral ventricle in hydrocephalus is much larger than normal when CSF flows. As a result, there is a significant statistical difference in the expansion of the ventricular for hydrocephalus. To employ the behaviour of CSF for hydrocephalic patients we use the following parameters Porosity (0.25), Pressure gradient (2700), Elasticity(350Pa), Reynolds Number (468.3), Womersley Number (more than 8.9) and Resistance parameter (1.367).The graphs shows velocity profile(cm/s) in y axis and Time 't' along x axis.

Fig 1 exploits the variation of the Reynolds number with time variation. Re varies from 130, 240,420 has been depicted for CSF with hydrocephalus subjects. Here it is shown that the velocity increases as the when Reynolds number escalates with time taken for cardiac cycle.

When the flow fluctuates during the early systole of the cardiac cycle, the velocity of CSF flow reaches a peak. When the frequency increases over time, the circulation rate of hydrocephalus reduces. As a result, increasing the Womersley number for pulsatile flow to 6.2, 7.5, or 8.9 with variable velocity yields the optimum volumetric flow rate. Fig: 4.

The greatest amount of hydrocephalus is reached in Fig 2 with varied Resistance parameters 0.9, 1, 1.36. Furthermore, when the fluid level increases, the ventricular flexibility deforms (see Fig 3). The brain parenchyma porosity is estimated to be 0.2 [4]. As a result, the fluid velocity increases as the permeability increases, demonstrating the elevated pressure of the CSF fluid flow.The pressure of hydrocephalus is close to 3000Pa whereas for normal subjects

is $\leq 500\text{Pa}$ [1]. We justify the increase in pressure graphically in Fig:5.

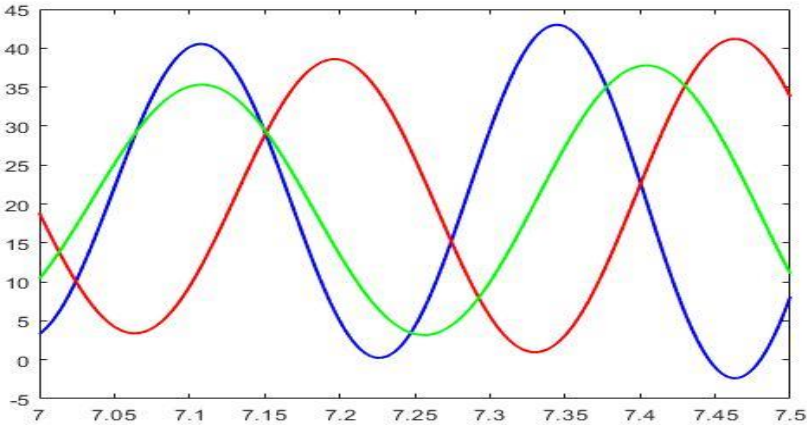


Fig: 1 Velocity profile with varying Reynolds number

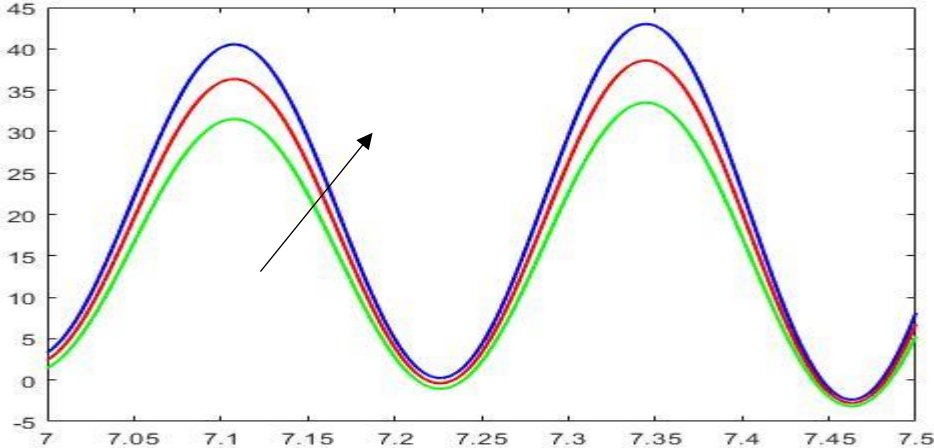


Fig: 2 Velocity profile with varying particle mass parameter

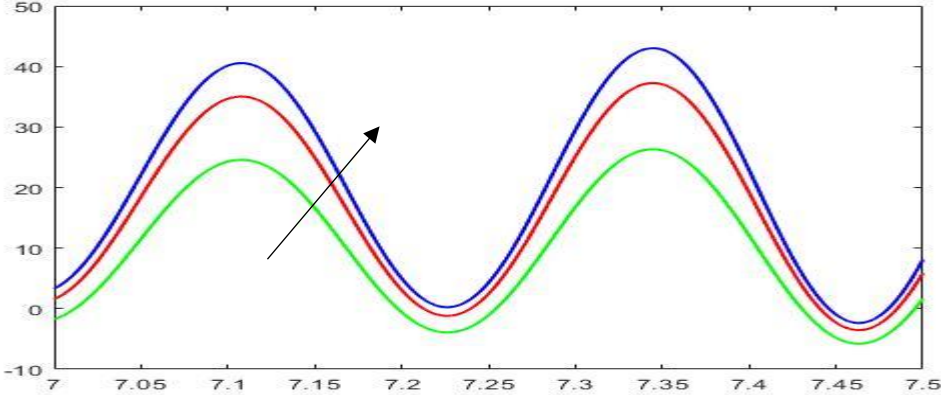


Fig: 3 Velocity profile with varying Elasticity

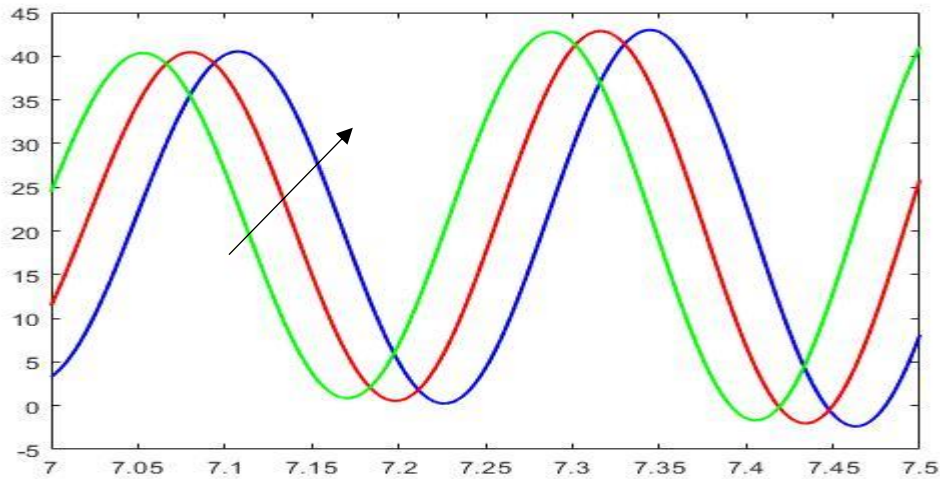


Fig: 4 Velocity profile with varying Womersley number

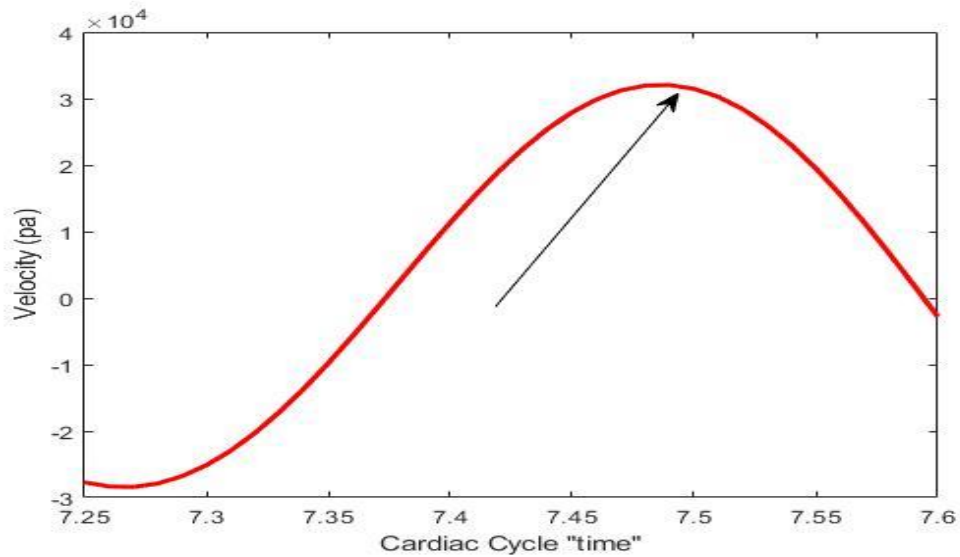


Fig: 5 Pressure of CSF from Velocity profile with varying with time 't'

CONCLUSION

In response to the impacts of high CSF pulsatile velocity, the hydrocephalus pressure differential in the brain fluctuates greatly. This leads to increased cranial system ventricular hypertrophy, as seen by the elasticity graph. When there is a rise in pressure, there is less ventricular compliance. CSF circulation as well as production will have an impact on the complete function of afflicted patients, resulting in brain damage.

The flow level in the cardiac cycle is predicted by important characteristics such as Womersley number α , elasticity G , and resistance parameter G_{pm} . This work verified a few noteworthy properties of fluid behavior in thermal transfer in a simplified representation of hydrocephalus useful for neurological studies. The following are the findings from the current study.

The momentum of fluid flow increases as the Darcy number, resistance parameter, Womersley number, and Reynolds number increase. Increased deformation (elasticity) caused by dimensional change increases cerebrospinal fluid velocity.

References

1. Gholampour, Seifollah, et al. "A mathematical framework for the dynamic interaction of pulsatile blood, brain, and cerebrospinal fluid." *Computer Methods and Programs in Biomedicine* 231 (2023): 107209.
2. Balasundaram, Hemalatha, et al. "Hydrocephalic cerebrospinal fluid flowing rotationally with pulsatile boundaries: A mathematical simulation of the thermodynamical approach." *Theoretical and Applied Mechanics Letters* 13.1 (2023): 100418.
3. Balasundaram, H., et al. "Effect of Ventricular Elasticity Due to Congenital Hydrocephalus. *Symmetry* 2021, 13, 2087." (2021).
4. Gholampour, S., et al. "Numerical simulation of cerebrospinal fluid hydrodynamics in the healing process of hydrocephalus patients." *Journal of Applied Mechanics and Technical Physics* 58 (2017): 386-391.
5. Linninger, Andreas A., et al. "Cerebrospinal fluid flow in the normal and hydrocephalic human brain." *IEEE Transactions on Biomedical Engineering* 54.2 (2007): 291-302.
6. Sweetman, Brian, et al. "Three-dimensional computational prediction of cerebrospinal fluid flow in the human brain." *Computers in biology and medicine* 41.2 (2011): 67-75.
7. Loth, Francis, M. Atif Yardimci, and Noam Alperin. "Hydrodynamic modeling of cerebrospinal fluid motion within the spinal cavity." *J. Biomech. Eng.* 123.1 (2001): 71-79.
8. Ambarki, Khalid, et al. "A new lumped-parameter model of cerebrospinal hydrodynamics during the cardiac cycle in healthy volunteers." *IEEE transactions on biomedical engineering* 54.3 (2007): 483-491.
9. Stadlbauer, Andreas, et al. "Insight into the patterns of cerebrospinal fluid flow in the human ventricular system using MR velocity mapping." *Neuroimage* 51.1 (2010): 42-52.
10. Gholampour, Seifollah. "FSI simulation of CSF hydrodynamic changes in a large population of non-communicating hydrocephalus patients during treatment process with regard to their clinical symptoms." *PloS one* 13.4 (2018): e0196216.
11. Chafi, M. Sotudeh, et al. "A finite element method parametric study of the dynamic response of the human brain with different cerebrospinal fluid constitutive

properties." *Proceedings of the Institution of Mechanical Engineers, Part H: Journal of Engineering in Medicine* 223.8 (2009): 1003-1019.